Advanced Wavefront Engineering for Improved Imaging and Overlay Applications on a 1.35 NA Immersion Scanner

Frank Staals, Alena Andryzhyieuskaya, Hans Bakker, Marcel Beems, Jo Finders, Thijs Hollink, Jan Mulkens, Angelique Nachtwein, Rob Willekers, (ASML Netherlands B.V.)
Peter Engblom (ASML Boise)
Toralf Gruner (Carl Zeiss SMT, GmbH)
Youping Zhang (Brion Technologies, Inc.; an ASML company)

ASML Netherlands B.V., De Run 6501, 5504 DR Veldhoven, the Netherlands

ABSTRACT

In this paper we describe the basic principle of FlexWave, a new high resolution wavefront manipulator, and discuss experimental data on imaging, focus and overlay. For this we integrated the FlexWave module in a 1.35 NA immersion scanner. With FlexWave we can perform both static and dynamic wavefront corrections. Wavefront control with FlexWave minimizes lens aberrations under high productivity usage of the scanner, hence maintaining overlay and focus performance, but moreover, the high resolution wavefront tuning can be used to compensate for litho related effects. Especially now mask 3D effects are becoming a major error component, additional tuning is required. Optimized wavefront can be achieved with computational lithography, by either co-optimizing source, mask, and Wavefront Target prior to tape-out, or by tuning Wavefront Targets for specific masks and scanners after the reticle is made.

Keywords: *Computational lithography, imaging, overlay, lens aberration control, mask 3D effects*

1. INTRODUCTION

Optical lithography has been one of the main drivers of semiconductor device shrink. Evolutionary optical design changes supported this shrinking resolution roadmap by enabling imaging at low wavelengths while maximizing lens numerical aperture (NA). The current generation semiconductor devices in volume production is based on 45 nm device architecture and use immersion lithography systems with 193 nm wavelength and 1.35 NA. The next major step in optical lithography will be EUV, introducing 13.5 nm wavelength, and starting with a 0.25 lens NA. Although EUV lithography is developing at high pace, for the near term 193 nm immersion lithography will remain the work horse for the critical layers in 32 nm and 22 nm technology nodes. Due to practical physical limitations in optics fabrication, lens NA cannot be further increased and novel technologies like source mask optimization (SMO) and double patterning technologies (DPT) are being used for the sub 45 nm devices.

Optical Microlithography XXIV, edited by Mircea V. Dusa, Proc. of SPIE Vol. 7973,
79731G · © 2011 SPIE · CCC code: 0277-786X/11/$18 · doi: 10.1117/12.880759

In previous papers 32 nm and 22 nm imaging resolution was demonstrated using various DPT methods [1,2]. Here we also discussed that DPT poses several new challenges to the lithography system, since both CD uniformity and overlay requirements are scaling stronger than with single exposure method. Additionally, the longer process cycle time, with double photo and etch steps, results in higher cost, which must be counteracted by increasing the productivity of the immersion scanners. All these new challenges have resulted in the introduction of a new immersion scanner platform which combines high productivity with low overlay. The latest generation TWINSCAN NXT™:1950i systems are capable of producing ~200 wafers per hour (wph) and have an overlay accuracy of ~2 nm, and the optical system used in this scanner is based on the proven 1.35 NA Zeiss optics. In a previous paper we presented the illumination extension with FlexRay™ function [3]. FlexRay is a concept using a micro mirror array to generate freeform illumination pupil shapes which in conjunction with SMO enables larger process windows. Additionally the illumination pupils can be tuned for proximity matching purposes, either to match different masks or different machines to each other. Results of Tachyon™ SMO and LithoTuner™ PatternMatcher are discussed in references [4] and [5], respectively.

This paper will discuss a further extension of the 1.35 NA optical system which uses a novel high resolution wavefront manipulator named FlexWave™. Lithography lenses have been equipped with lens manipulators for more than 15 years, but the number and accuracy of them has changed considerably over the years. Originally the correction capability was limited to magnification adjustments, but steadily the correction means have been increased over the generations. Modern scanners have many manipulators which aim to minimize the total lens aberration in a dynamic manner. The lens total wavefront aberration is expressed in an orthogonal Zernike series and the individual Zernike coefficients (up to Z36) are used to quantify the lens performance. With FlexWave higher order aberration terms can be adjusted and the Zernike series expansion is increased to include up to 64 Zernikes. Wavefront control with FlexWave minimizes thermal lens aberrations under high productivity usage of the scanner, hence maintaining overlay and focus performance. Additionally, wavefront tuning with FlexWave is possible, and we have been studying wavefront tuning to compensate for process induced effects, like compensating mask 3D effects which induce feature dependent focus shifts and pattern shifts. The FlexWave functionality is accompanied by Tachyon based computational solutions optimizing process window and minimizing focus shift and pattern shift.

The outline of the paper is as follows: In section 2 we present the basic concept of the FlexWave manipulator and its control, and show the wavefronts that can be introduced. In section 3 we discuss the mask 3D effects one can expect with high NA polarized imaging and explain how FlexWave may help in minimizing these effects. In section 4 we present the results of our scanner evaluation showing experimental data on imaging and overlay using FlexWave in the lens heating control, and finally in section 5 we summarize our conclusions.

2. FLEXWAVE MANIPULATOR

The FlexWave manipulator consists of an optical element positioned close to a pupil plane of the projection lens. It is heated locally through tiny conductive and resistive structures. These structures are small enough to keep effects of obscuration and scattering negligible, so that there is no negative impact on imaging. The element is cooled in parallel to ensure a consistent control as well as thermal neutrality against surrounding lens elements. The principle of the FlexWave manipulator is illustrated in figure 1, depicting a plane-parallel optical plate with heating zones. The principle can also be applied to lenses and mirrors.

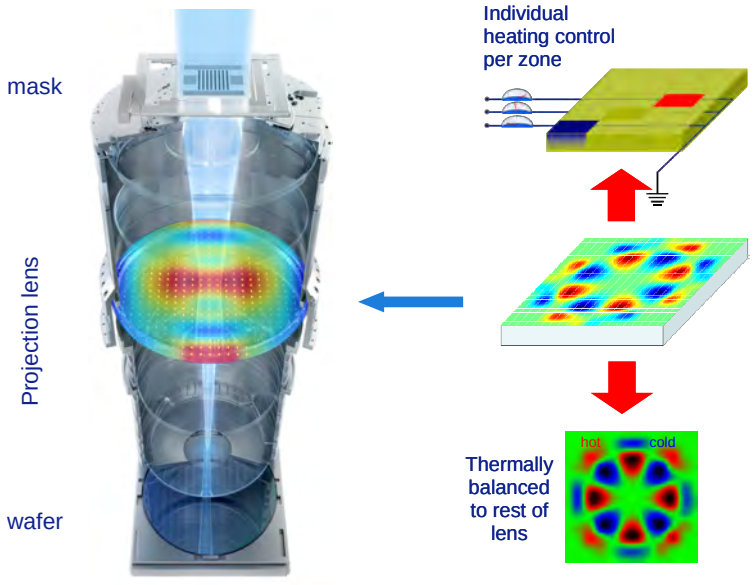

Figure 1: The principle of the FlexWave manipulator: an optical element close to a pupil plane of the projection lens, illustrated here by a plane-parallel optical plate which has a 2D matrix with heating zones.

In quartz at 193 nm wavelength, an increase in temperature of 1 K leads to an increase in the refractive index, translating into 20 nm change in optical path length per mm material. In negative sense this effect is responsible for thermal aberrations (lens heating), but we can use it positively to improve the wavefront by actively steering a desired temperature profile. This is done by individually adjusting the electrical power fed into the heating segments. For the component as a whole, heating and cooling power are balanced. In addition, the temperature at each thermal contact point is actively controlled to match the lens temperature.

The FlexWave user interface and metrology software are 64 Zernike based. At module level the Zernike steering is translated into local heating power. Based on a detailed hardware model the software can optimize to actual hardware capability, and predict the wavefront that will be achieved. Because FlexWave is a (near) pupil lens element it can correct best for Zernike offsets. In figure 2 we present the results of a wavefront set-get experiment for each individual Zernike.

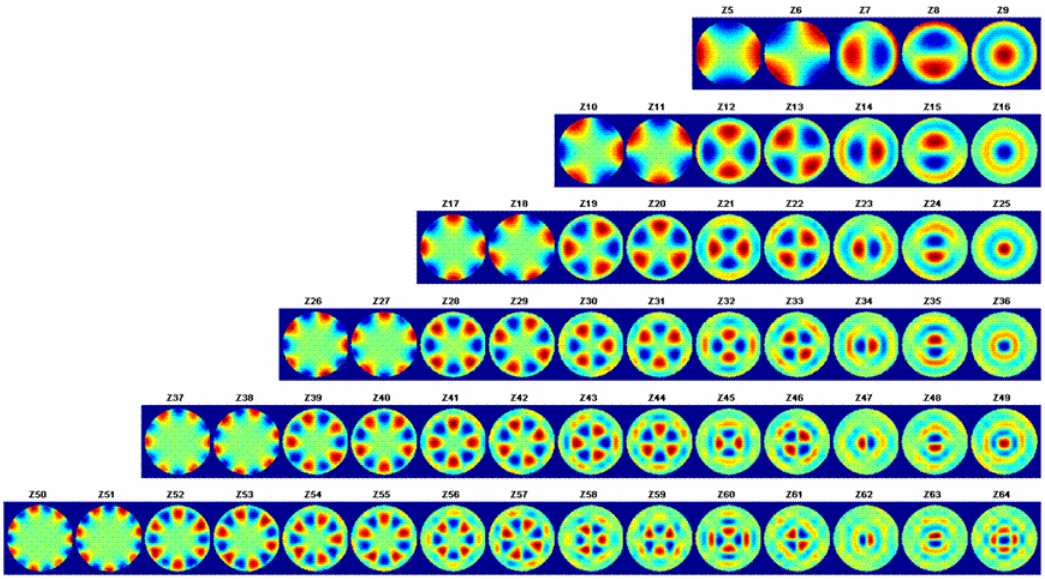

Figure 2: FlexWave response to the 64 Zernike settings as measured in a scanner system with a 1.35 NA immersion lens

3. MASK 3D EFECTS AND IMAGING ENHANCEMENT

Historically lithography simulations were based on the Kirchhoff approximation, which assumes a 2D thin mask grating in the object plane. Starting with the 45 nm node, mask features have dimensions smaller than the optical wavelength of 193 nm (on 4x systems). With ever decreasing feature sizes and increasing mask absorber aspect ratios, the three dimensional (3D) structure can no longer be neglected, and Kirchhoff approximation has to be replaced by a rigorous simulation, which takes into account the wave's optical behavior near the mask. The mask 3D effect results in feature dependent focus and pattern shift, and CD asymmetries.

The Tachyon M3D tool is a fast and approximate method to simulate mask 3D effects for full chip applications [6]. Comparison to measurement results is shown in figure 3, this for a 22 nm SRAM contact layer example. The magnitude of the mask 3D induced effects depends on the exact absorber stack design and the mask processing tolerances on especially side wall angle. However, even with well-chosen materials and highly accurate mask manufacturing control significant residual effects are expected [7] [10] [11].

In figure 4 we present a sensitivity analysis on the mask 3D effects. The absorber thickness causes the best focus to become dependent on pattern pitch. It is shown that for absorber thickness of 70 nm the effect in focus shift can be 50 nm. Side wall angle effects in the chrome absorber stack may cause pattern asymmetries. For a two bar pattern we calculate that CD differences can 0.6 nm for 20 degree side wall angle errors.

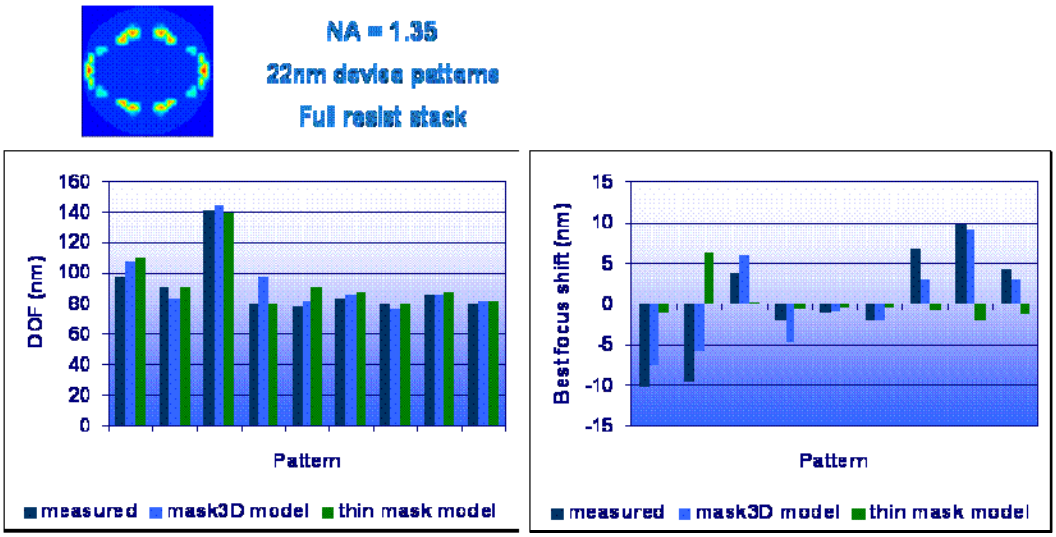

Figure 3: Comparing the measured DOF and best focus with simulated results using either the M3D Tachyon function or using the Kirchof approach. This is done for a 22 nm SRAM pattern.

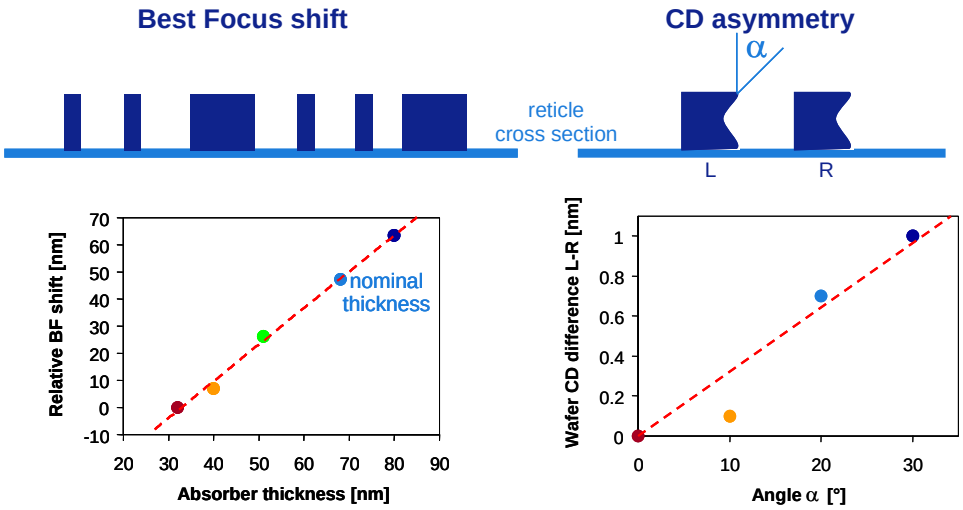

Figure 4: Sensitivity of focus shift and CD asymmetry for mask 3D effect caused by the absorber stack thickness and stack geometry.

A possible way to reduce the mask 3D effects is to apply wavefront tuning with FlexWave. A Wavefront Target setting can compensate focus and/or pattern shifts. The optimization principle is explained in figure 5. Small structures (core) shift in focus due to local radial phase tilt (global curvature over their diffraction orders), large structures (periphery, overlay marks) shift in focus due to local curvature around their zeroth order. Small structures shift in XY due to asymmetric offsets (global tilt), large structures due to local tilt around their zeroth order. A pure pattern shift is created if the total area of all diffraction orders of a feature sees the same wavefront tilt. In case of overlapping

diffraction orders (which will practically always be the case), desired and undesired effects of wavefront tuning must be balanced. All (critical) features on a mask should be included in that evaluation.

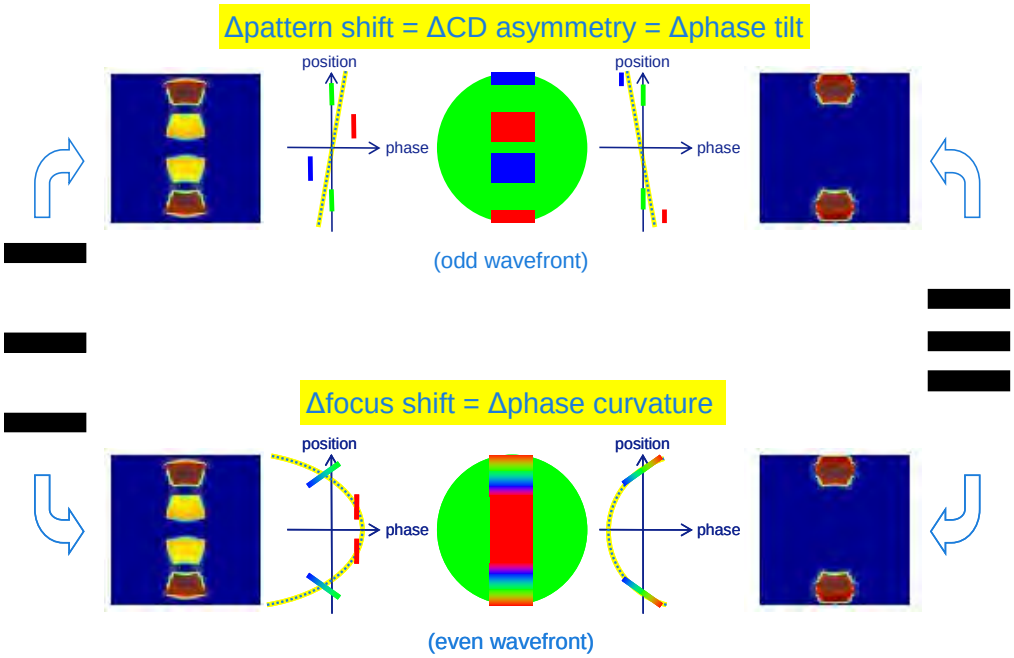

Figure 5: Basic principles of applying feature dependent pattern shift or focus shift.

In order to evaluate to what extend FlexWave can help to reduce mask 3D effects we have been doing some computational and experimental evaluation. The computational evaluation is based on a 22 nm SRAM pattern, while the experimental evaluation was done for a 45 nm NAND pattern.

3.1 Computational Optimization of wavefront

Determining the Wavefront Target for a given layer design is challenging and requires computational optimization algorithms with knowledge of both the mask design and the scanner lens model. The Tachyon computational lithography platform allows running sophisticated optimization algorithms to find the best solution. There are two possible optimization flows thinkable: 1) Wavefront optimization in conjunction with source mask optimization, and 2) wavefront optimization for a given mask and illuminator pupil. In figure 6 we present a comparison of these optimization flows, and here it is illustrated that the first optimization flow is suitable for the pre-tape out mask design phase, whereas the second optimization flow is suitable for wavefront tuning in the wafer manufacturing environment.

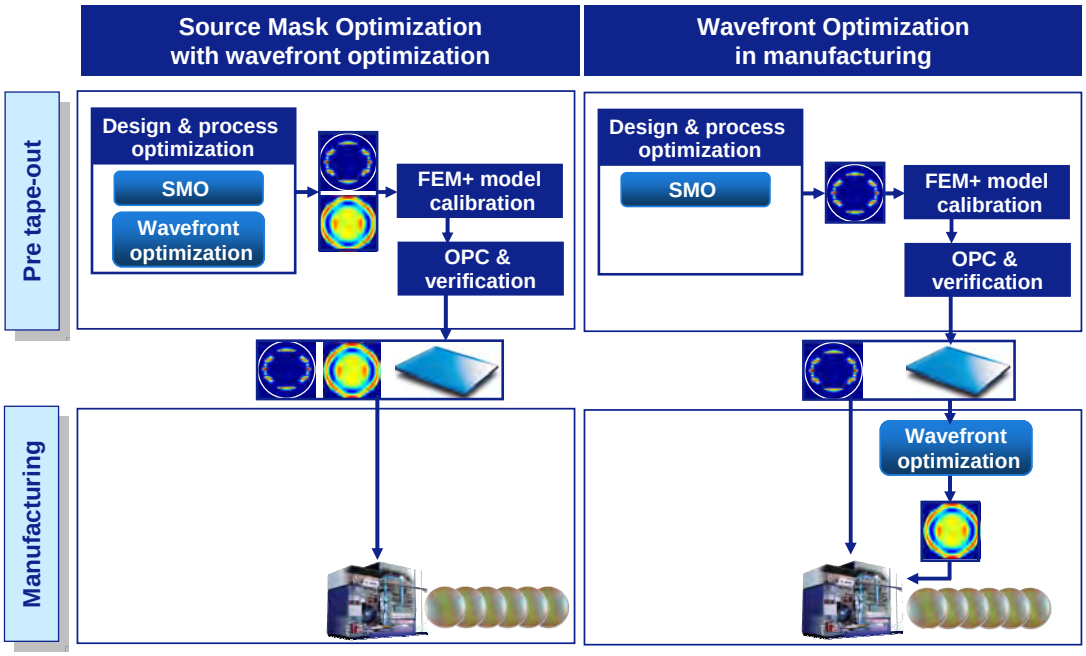

Figure 6: Two possible optimization flows: on the left pre-tape-out wavefront optimization, which is done in conjunction with SMO, and on the right optimization in the manufacturing phase for a given mask and source design.

As part of our wavefront tuning feasibility study we have been evaluating a 22 nm design SRAM contact structure, using SMO with wavefront tuning. In the Tachyon computational model we minimize the edge placement error (EPE) of the critical cut-lines in of the SRAM structure, and we compare the resulting across field process window for the optimization with FlexWave to an SMO optimization without FlexWave tuning. The results presented in figure 7 show that SMO with FlexWave increases the process window for focus by 9%.

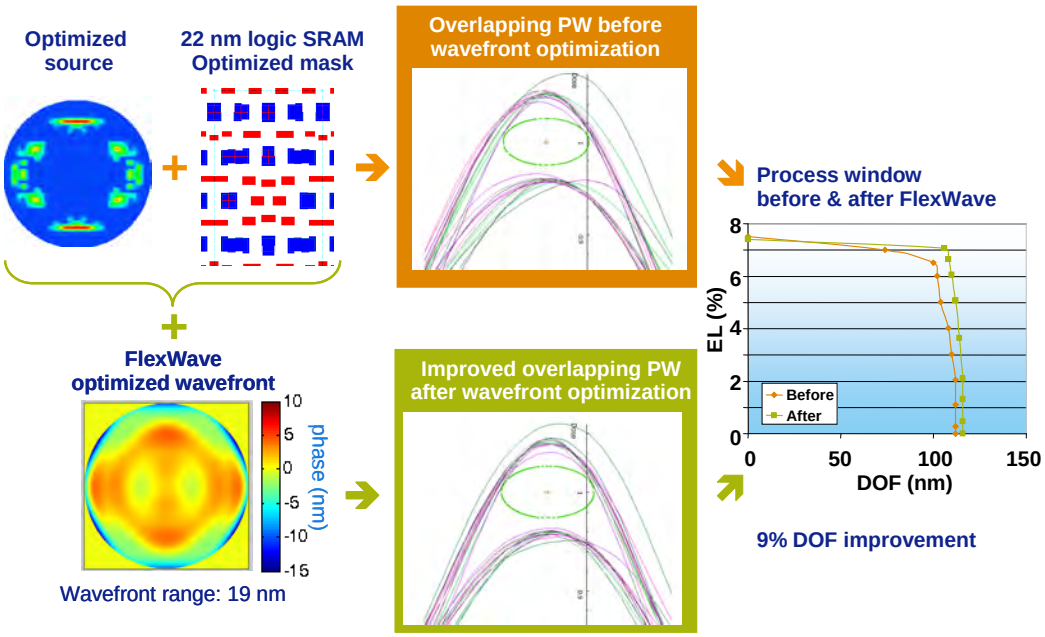

Figure 7: Comparing process windows of a 22-nm SRAM contact layer, once optimized with SMO only, and once optimized with SMO and FlexWave. The latter shows 9 % DOF increase.

3.2 Experimental Optimization of wavefront

For the experimental optimization we used an ASML test reticle with critical NAND patterns. In figure 8 we show these patterns. The NAND core structure is a vertical 45 nm symmetric line space structure, the word lines (WL) of which are sensitive for mask 3D induced CD asymmetry effects (top CD minus bottom CD, or T-B). The periphery structures are both horizontal and vertical lines with wider pitch and CD range. These structures will show a best focus shift caused by mask 3D effect.

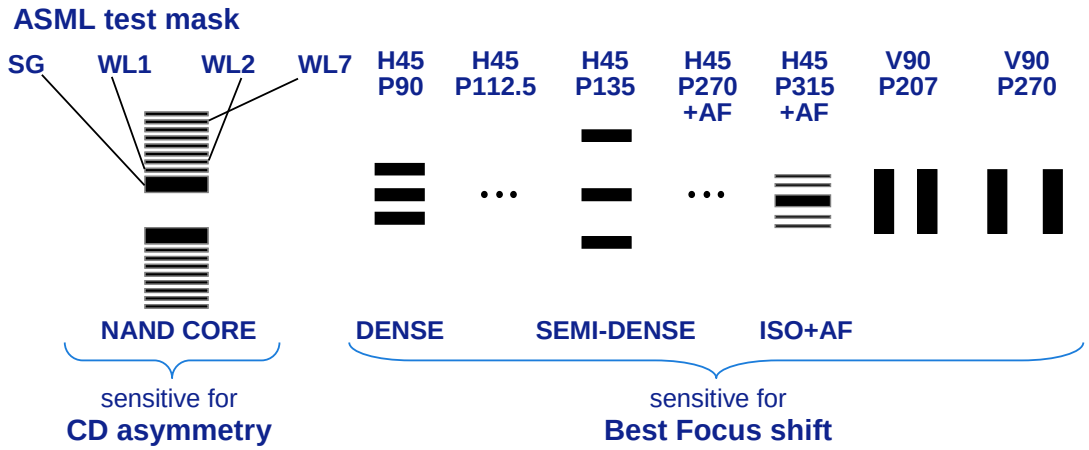

Figure 8: NAND patterns as put on the reticle for the experimental test case; patterns are sensitive for mask 3D focus shift effect and CD asymmetry effect

The optimization of the wavefront was targeted to minimize both T-B and best focus shift of each individual pattern simultaneously. In figure 9 we present the results of the optimization and compare the results with the one of a non-optimized case. The result shows that best focus shift is reduced from 34 nm to 18 nm and T-B is reduced from 1.3 nm to 0.7 nm. It also should be noticed that co-optimization of best focus with T-B gives similar improvement result as when optimizing only for best focus or T-B, so it can be concluded that optimization of both artifacts can be done quite independently (even versus odd wavefront components).

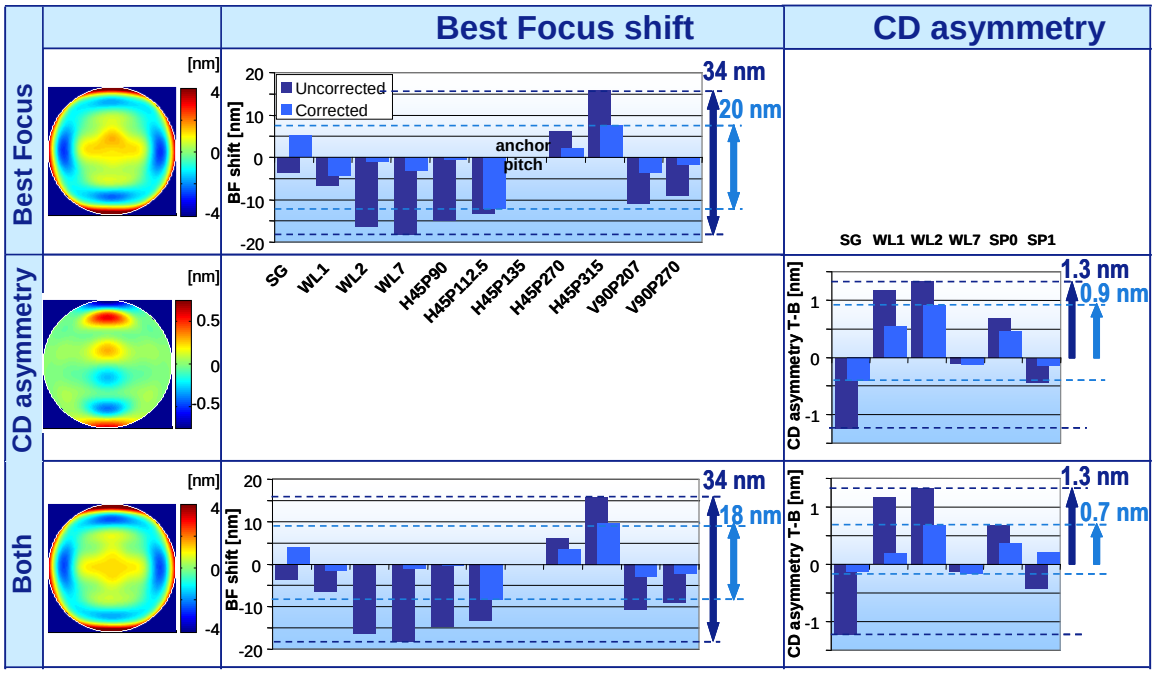

Figure 9: Experimental results of the best focus and CD asymmetry optimization of the NAND case.

4. FLEXWAVE CONTROL FOR HIGH PRODUCTIVITY PERFORMANCE

Cost of ownership (COO) reduction is the main driver of lithography, and one of the parameters determining COO is the productivity of the scanner. For the 1.35 NA immersion systems, productivity since 2007 has been increased from ~130 wph to ~200 wph. The heat load in the optical system scales with system productivity, and thus with increasing wafers per hour improvements are needed in the control of the thermal aberrations [8,9]. FlexWave is the ultimate step in thermal aberration control. FlexWave correction is faster than the heating behavior of the projection lens, and increases the correction potential of the lens more than a factor 2. In figure 10 we present simulated lens heating evaluation results for different use cases, whereas in figure 11 experimental results are presented for a DRAM use case. Here we used a TWINSCAN NXT:1950i

system equipped with FlexWave running a FEM wafer with DRAM structures. The reticle transmission was 25%, the illumination setting rotated dipole with 30 degree opening angle, and the expose dose 24.4 mJ/cm^2. The experimental data confirms the theoretical prediction of improved correction potential of more than a factor 2.

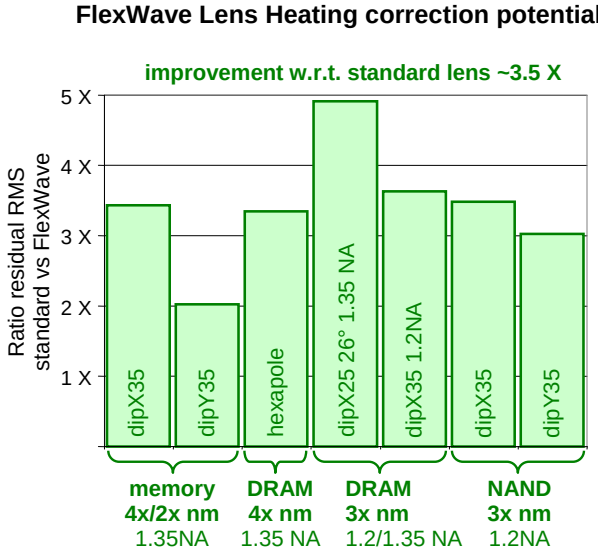

Figure 10: Lens heating correction potential improvement of a lens with FlexWave compared to a lens without FlexWave; evaluation for 7 different use cases based on simulation

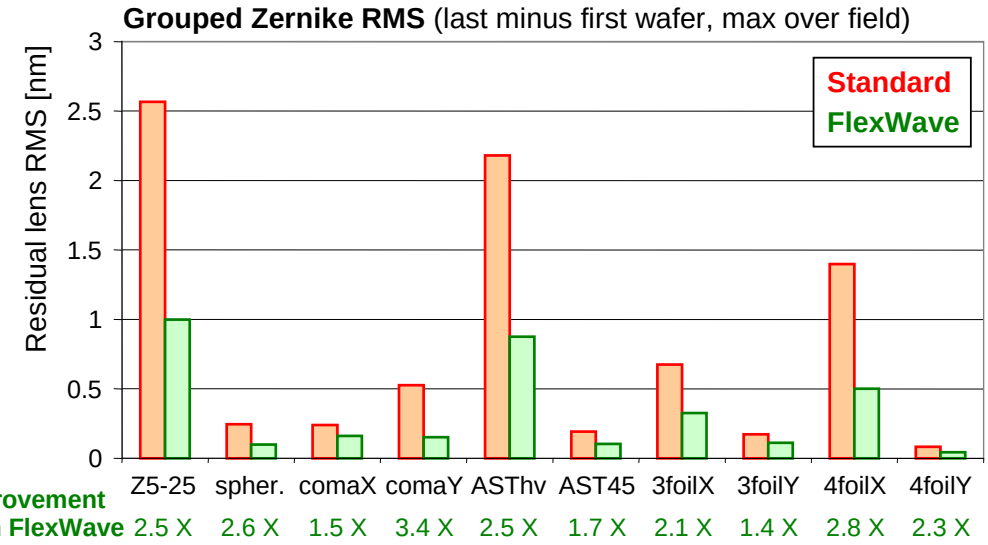

Figure 11: Experimental comparison of residual aberrations after aberration control for a standard 1.35 NA lens and a lens equipped with FlexWave

The improvement in thermal aberrations will result in through lot improvements of both overlay and imaging. In figure 12 we show the CD values of 3 different features on the FEM wafers used for figure 11. One of them is sensitive to the lens heating induced aberrations and drifts over the lot. The drift gets twice as low with FlexWave control.

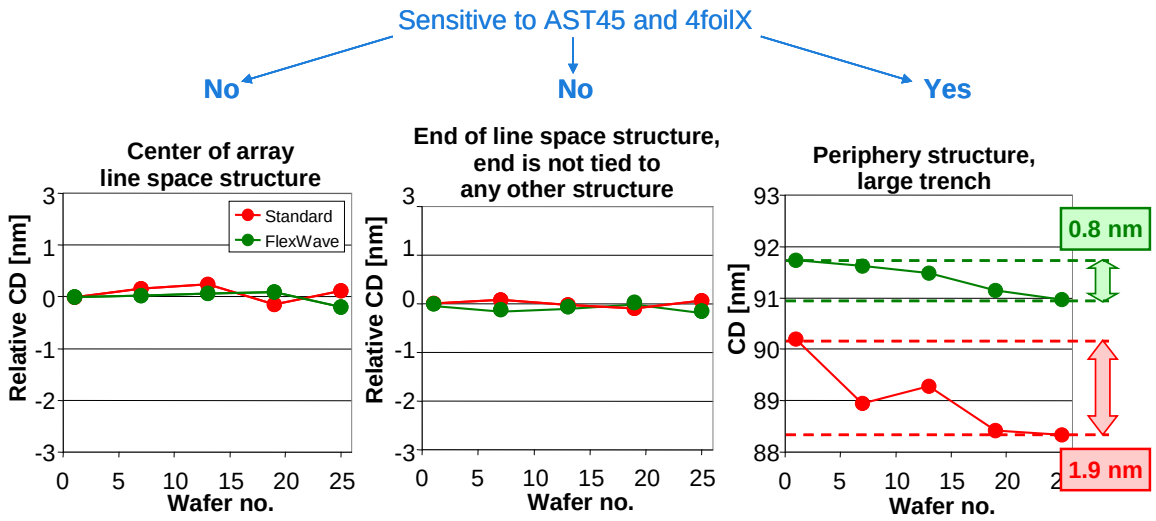

Figure 12: Full lot CD analysis, showing more than a factor 2 reduction of CD drift with FlexWave.

Overlay improvement was evaluated for a worst case test in which the both layers are exposed under very different conditions. Layer 1 was exposed with a low transmission mask, under annular illumination, unpolarized and at 30 mJ/cm^2 exposure dose. Layer 2 was exposed with a high transmission mask, under dipole X illumination, polarized and at 50 mJ/cm^2 exposure dose. Overlay was measured with Box-in-Box (BiB) targets. The overlay comparison with and without FlexWave is presented in figure 13. The full lot overlay is reduced from 8.3 nm to 5.3 nm when using FlexWave in a dynamical aberration control mode.

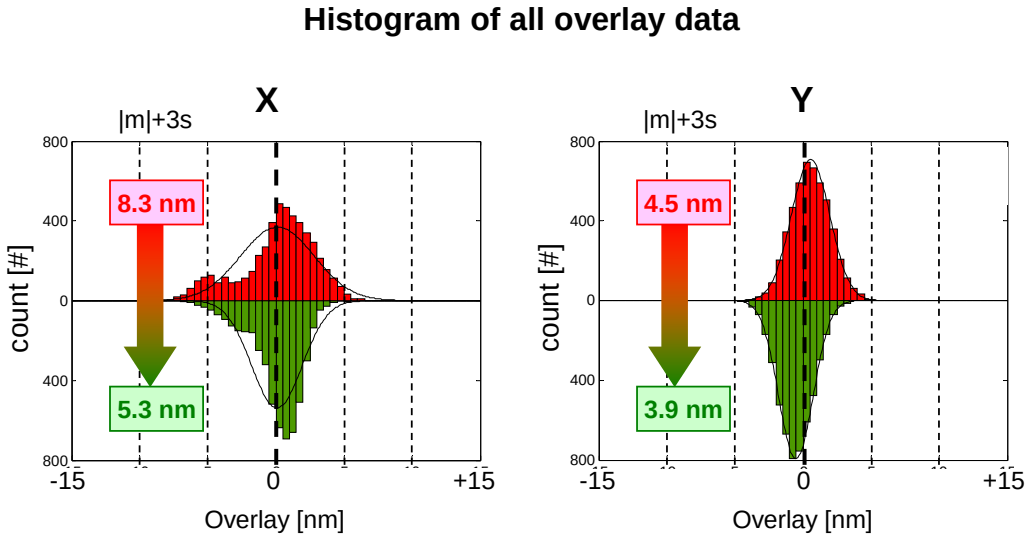

Figure 13: Full lot overlay analysis of our worst case overlay tests, showing 3 nm through lot overlay improvement with FlexWave.

5. CONCLUSIONS

In this paper we introduced a novel high resolution wavefront manipulator named FlexWave. FlexWave is an optical extension of the 1.35 NA lithography lens used in the TWINSCAN NXT:1950i immersion scanner. Next to improvements in thermal aberration control, the FlexWave can be used for imaging enhancements which minimize mask 3D effects.

For thermal lens aberration control we presented simulation and experimental results showing that with FlexWave the correction potential for different use cases is improved with more than a factor 2, which is well in line with the systems productivity roadmap. The dynamic lens heating control resulted in 3 nm through lot overlay improvement for an overlay test in which the two layers were exposed under very different conditions. CD performance over lot was improved by 1 nm.

FlexWave in the imaging enhancement mode is being studied to minimize mask 3D effects. We studied a 22 nm SRAM contact layer case with computational lithography and observed a 9% increase in DOF. For NAND test structure we did an experiment to reduce the best focus difference between the different test structures and to reduce the CD asymmetry of the NAND core structure. Here we found a reduction in best focus differences of 16 nm and a reduction in CD asymmetry of 0.6 nm.

ACKNOWLEDGEMENTS

We would like to than Craig Hickman, Scott Light, Jianming Zhou of Micron Technology for providing customer case measurement data.

REFERENCES

[1] Jo Finders et.al, “Double patterning lithography for 32 nm: critical dimensions uniformity and overlay control considerations”, J. Micro/Nanolith. MEMS MOEMS 8, 011002 (2009)

[2] Jo Finders et.al, “Litho and patterning challenges for memory and logic applications at the 22-nm node”, Proc. SPIE 7640, 76400C (2010)

[3] Melchior Mulder et.al, “Performance of FlexRay: a fully programmable illumination system for generation of freeform sources on high NA immersion systems”, Proc. SPIE 7640, 76401P (2010)

[4] Robert Socha et.al, “Design compliant source mask optimization (SMO)”, Proc. SPIE 7748, 77480T (2010)

[5] Robert Socha, “Improved fab CDU with FlexRay and LithoTuner”, Proc. SPIE 7973, paper 25 (2011)

[6] Peng Liu et al., “Fast and accurate 3D mask model for full-chip OPC and verification”, Proc. SPIE 6520, (2007)

[7] Jo Finders, Thijs Hollink, “Mask 3D effects: impact on Imaging and Placement”, Proc. EMLC 27, (2011)

[8] Igor Bouchoms et.al, “Advanced imaging with 1.35 NA immersion systems for volume production”, Proc. SPIE 7640, 76401R (2010)

[9] Tom Castenmiller et.al, “Towards ultimate optical lithography with NXT:1950i dual stage immersion platform”, Proc. SPIE 7640, 76401N (2010)

[10] Johannes Ruoff, Jens Timo Neumann, Emil Schmitt-Weaver, Eelco van Setten, Nicolas le Masson, Chris Progler, Bernd Geh, “Polarization-induced astigmatism caused by topographic masks”, Proc. SPIE 6730, (2007)

[11] A. Erdmann, F. Shao, P. Evanschitzk, and T. Fühner, “Mask-topography-induced phase effects and wave aberrations in optical and EUV lithography”, Journal of Vacuum Science and Technology B: Microelectronics and Nanometer Structures 28, C6J1 (2010)